HHS Public Access

Author manuscript

Heart Rhythm. Author manuscript; available in PMC 2021 June 01.

Published in final edited form as:

Heart Rhythm. 2020 June ; 17(6): 1025–1033. doi:10.1016/j.hrthm.2020.02.007.

Mechanisms of atrial fibrillation in aged rats with heart failure with preserved ejection fraction

Thassio Ricardo Ribeiro Mesquita, PhD[1,*], **Rui Zhang, MD**[1,2,*], **Geoffrey de Couto, PhD**[1], **Jackelyn Valle, BS**[1], **Lizbeth Sanchez, BS**[1], **Russell G. Rogers, PhD**[1], **Kevin Holm, BS**[1], **Weixin Liu, MS**[1], **Eduardo Marbán, MD, PhD**[1], **Eugenio Cingolani, MD**[1]

[1]Smidt Heart Institute, Cedars-Sinai Medical Center, Los Angeles, California, USA.

[2]Department of Cardiology, Xinhua Hospital, Shanghai Jiaotong University, School of Medicine, Shanghai, China.

Abstract

Background: Although ~20% of the elderly develop atrial fibrillation (AF), little is known about the mechanisms. Heart failure with preserved ejection fraction (HFpEF), which is associated with AF, is more common in aged females than in males.

Objective: To identify potential mechanisms of AF in an age-related HFpEF model.

Methods: In aged (21–24-month-old) female Fischer F344 rats, which are prone to HFpEF, we induced AF by atrial pacing. Young Fischer F344 (3–4-month-old) and age-matched Sprague Dawley rats (27-month-old) female rats served as controls. Phenotyping included echocardiography to assess left ventricular (LV) structure/function; *in vivo* electrophysiology and *ex vivo* high-resolution optical mapping to assess AF vulnerability; systemic and atrial inflammatory profiling; atrial histology; and expression of inflammasome signaling proteins.

Results: Aged rats developed LV hypertrophy, left atrial enlargement, diastolic dysfunction, and pulmonary congestion, without EF impairment, thus meeting the criteria for HFpEF. Increased serum inflammatory markers, hypertension, and obesity further characterize aged females. Sinoatrial and atrioventricular node dysfunction were associated with high inducibility of AF in aged rats. *Ex vivo* electric activation mapping revealed abnormal β-adrenergic responsiveness and slowed conduction velocity. Atrial inflammasome signaling was enhanced in aged rats, which may contribute to fibrotic remodeling and high AF susceptibility.

Conclusions: Together, our data demonstrate that aging-related atrial remodeling and HFpEF are associated with atrial enlargement, fibrosis, conduction abnormalities, and nodal dysfunction, favoring a substrate conducive to AF.

Address for correspondence: Eugenio Cingolani, MD, Smidt Heart Institute, Cedars-Sinai Medical Center, 127 S. San Vicente Blvd., Los Angeles, CA 90048, eugenio.cingolani@csmc.edu.

*These authors equally contributed to this work

Conflicts of Interest: none.

GRAPHICAL ABSTRACT

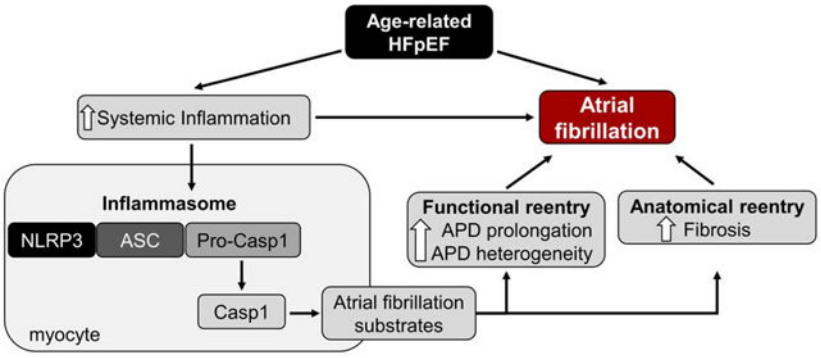

Keywords

atrial fibrillation; aging; HFpEF; inflammation; fibrosis

INTRODUCTION

Heart failure with preserved ejection fraction (HFpEF) is increasingly common, notably in the elderly population, and is highly associated with atrial fibrillation (AF)[1,2]. Epidemiological studies reveal women outnumber men in the prevalence of HFpEF[3,4]. Furthermore, comorbidities such as hypertension, obesity, diabetes mellitus, and renal dysfunction may facilitate the development of AF in HFpEF patients[2,5]. Unlike HF patients with reduced EF, where multiple pharmacological agents and device-based therapies have been shown to improve survival, therapeutic options for patients with HFpEF are limited to symptomatic relief[5–7]. Prognosis remains poor, with a median survival of ≈2 years and 5-year mortality of ≈75%[8]. Therefore, identification of molecular mechanisms involved in the pathophysiology driving AF in HFpEF is of paramount importance to guide the development of future therapies. Here, we demonstrate AF is highly prevalent in aged female rats with echocardiographically-verified diastolic dysfunction and objective signs of HF. Moreover, atrial enlargement and fibrosis may favor a substrate conducive to AF.

METHODS

All animal experiments were approved by the Cedars-Sinai Institutional Animal Care and Use Committee and performed in compliance with the Guide for the Care and Use of Laboratory Animals proposed by the Institute of Animal Resources and published by the National Institutes of Health. Young female Fischer 344 rats (3 ± 1-month-old) were purchased from Envigo (Indianapolis, IN, USA) and old female Fischer 344 rats (21 ± 3-month-old) were obtained from the NIH/NIA aging colony. Old female Sprague Dawley rats (27-month-old), which are not prone to HFpEF, served as age-matched controls. Transthoracic echocardiography was used to assess systolic and diastolic function evaluated by the parasternal short-axis and apical 4-chamber (pulse-wave Doppler mode) views, respectively[9].

Programmed electrical stimulation (PES) was performed using a 1.2 French octapolar electrophysiology catheter (Millar Instruments) inserted into the right atrium via the jugular vein, as described[10]. AF was induced by atrial burst pacing, starting with 2 second burst pacing at a cycle length of 40 ms and decreasing in each successive burst by a 2 ms reduction to a cycle length of 10 ms. AF was defined as the occurrence of rapid, fragmented atrial electrocardiograms with irregular R-R intervals lasting ≥1 second. Flow cytometry was carried out on white blood cells, as described[11]. Inflammatory cytokines were quantified using commercially available cytokine array kits.

In vivo heart rate (HR) response to β-adrenergic receptor (β-AR) stimulation was measured in anesthetized rats. High-resolution voltage maps and electrograms were acquired simultaneously in isolated intact SAN/atrial tissue loaded with a voltage-sensitive dye. Electrograms were recorded using three electrodes, immersed in the bath in close proximity to reduce electrical impedance. Fibrosis was evaluated in left atrial (LA) tissue by Masson's trichrome staining. Protein expression of inflammasome targets was assessed in LA by western blot. The Online Supplement provides additional methodological details (Supplemental Methods).

Pooled data are expressed as means ± SEM. Statistical comparisons were performed using GraphPad Prism 6 (San Diego, CA, USA), with significance determined using a two-tailed unpaired Student's t-test. Concentration-effect relationships were analyzed by sigmoidal fits generated to calculate the half-maximal effective (EC50) and inhibitory (IC50) concentrations. For comparisons of AF incidence, a 2 × 2 contingency table using $\chi 2$-test without Yates correction was used. $P<0.05$ was considered statistically significant.

RESULTS

Aging-related diastolic dysfunction associated with proinflammatory stress

To determine whether aged females develop diastolic dysfunction with preserved EF, all animals underwent initial screening by echocardiography. As shown in Figure 1A, EF remained unchanged between young and old animals. In contrast, analysis of E- and A-wave changes from pulse-wave Doppler mode, and E'- and A'-wave changes in tissue Doppler, revealed diastolic dysfunction as evidenced by decreased E/A ratio (Figure 1B) and increased E/E′ ratio (Figure 1C). Table 1 summarizes echocardiographic and anatomic measurements in the two groups. Diastolic dysfunction does not suffice to diagnose HFpEF: signs of HF must be present. We verified that lung weight/body weight ratio was elevated in aged rats (Figure 1D), indicative of pulmonary congestion. Cardiac hypertrophy was evident from the steady increase of LV diameter, along with augmented cardiac weight (Table 1), which were associated with elevated blood pressure in aged female rats (Figure 1E). Age-associated HR reduction was accompanied by prolonged PR, QRS, and QT intervals on ECG (Figure 1F). Consistent with common features of HFpEF patients, aged animals presented increased atrial weight, an indication of atrial hypertrophy, and excessive accumulation of adipose tissue (Table 1). Finally, exercise capacity was impaired in aged animals (Table 1), consistent not only with HF but also with the skeletal myopathy that has been described in obese HFpEF rats[12]. Animals with normal diastolic function, reduced EF,

and/or no evidence of HF signs were excluded and omitted from all analyses mentioned above (~10% of cases).

As age-matched control rats, we used female Sprague Dawley rats, which are not prone to diastolic dysfunction in an age-dependent manner. As shown in the Supplemental Figure 1A, EF remained unchanged in both aged rat strains, while diastolic function was significantly impaired in aged Fischer 344 rats but not compared in aged Sprague Dawley rats (Supplemental Figure 1B–C).

In various models of HFpEF, inflammation has been observed, both systemically and in the heart[7,13]. Here, we show that age-related HFpEF is associated with a remarkable increase in CD11b+ cells (a leukocyte marker) and granulocytes, while no differences were observed in peripheral T cell populations (CD4/CD8) (Figure 1G–H). Quantification of cytokines in the serum confirmed higher levels of proinflammatory and profibrotic cytokines in senescent rats compared with young rats (Figure 1I). Among those cytokines, some have been linked to the development of HFpEF, including monocyte chemotactic protein-1 and C-X-C motif chemokines[7,14]. On the other hand, lower circulating levels of IL-6 and IL-10 were found in aged females compared with young animals. Underlying the increase in obesity, leptin levels were elevated in aged rats (Figure 1I).

Atrial enlargement and SAN/AV dysfunction in aged rats

Consistent with the earlier findings of atrial hypertrophy echocardiography confirmed enlargement of the LA in aged animals compared with young (Figure 2A). The severity of diastolic dysfunction correlates with LA enlargement (Figure 2B). P wave duration was also prolonged in aged compared to young animals (Figure 2C). To further assess sinoatrial node (SAN) and atrioventricular (AV) function, and AF inducibility, we performed PES. Aged animals showed longer cSNRT than young rats, indicating intrinsic SAN dysfunction (Figure 2D). In accordance with longer PR intervals (Figure 1F), aged animals also displayed AV node dysfunction as identified by increased 2:1 AV node conduction cycle length (Figure 2E) and Wenckebach cycle length during invasive electrophysiology study (Figure 2F). Aged animals also presented prolonged atrial effective refractory period (AERP) compared to young animals (Figure 2G). To test whether these changes promote higher susceptibility to developing AF, we applied an overdrive atrial pacing protocol (Figure 2H, left). Supporting our hypothesis, no AF was recorded in young animals, whereas a remarkable increase was found in aged rats (Figure 2H, right). Only one animal developed sustained AF (>1800 sec), while the others had self-terminating AF lasting <30 sec (Figure 2I). Further substantiating our findings, age-matched controls validated the prolonged AERP in aged HFpEF animals (Supplemental Figure 1D), which was linked with higher AF inducibility (Supplemental Figure 1E). Although only one non-HFpEF aged animal developed AF, its duration was very brief (<10 sec) compared with HFpEF animals (Supplemental Figure 1F).

Chronotropic reserve in aged rats

Chronotropic incompetence is characteristic of HFpEF[5]. *In vivo* β-AR pharmacological stimulation (Figure 3A) revealed a significant increase in maximum HR in both young and

old groups (Figure 3B–C), but the fractional increment was attenuated in older animals, indicative of diminished chronotropic reserve (Figure 3D). Analysis of HR recovery revealed a similar decay time in the two groups (Figure 3E).

Slow conduction potentiates arrhythmia in aged rats

Autonomic imbalance has been shown with advanced age, contributing to impaired pacemaker function and AF[15]. To exclude contributions from autonomic innervation, we studied excised SAN/atrial preparations. Figure 4A shows representative data: a typical specimen with surrounding electrodes (left panel), and simultaneous electrograms and optical signals in young and old rats (middle and right panels). These examples show differing responses to a submaximal concentration of isoproterenol (Iso, 10 nmol/L) in the young and old SANs. Pooled data reveal a rightward shift in chronotropic responsiveness to Iso in aged animals, but unchanged maximal responses (Figure 4B). In addition to increasing HR, β-AR stimulation abbreviates action potential (AP) duration[16,17]. Optical AP recordings of the LA revealed a longer AP duration at 90% repolarization (APD_{90}) at baseline in old specimens. At high doses (≥100 nmol/L) of Iso, APD_{90} converged to the same value (~40 ms) in old and young specimens, but, once again, there was a rightward shift, with old being less sensitive than young at intermediate doses (Figure 4C).

Representative activation maps demonstrate that, in sinus rhythm, the earliest activation site is located at the right atrial posterior wall, which anatomically corresponds to the location of the SAN and then spreads throughout the atria (Figure 4D). Conduction velocity (CV) at baseline is faster in young than old; with cumulative concentrations of Iso, CV goes up in both groups, but more modestly in the aged atria (Figure 4E). During β-AR stimulation, 80% of aged specimens developed irregularities of rhythm (e.g., bigeminy or bursts), while none of the young animals showed such irregularities (Figure 4F).

Atrial fibrosis and atrial fibrillation in aged rats

In accordance with slowed conduction, Masson’s trichrome staining revealed increased LA fibrosis in aged animals compared to young (Figure 5A). The heterogeneity of APD_{90} was significantly higher in aged animals (Figure 5B), and such heterogeneity correlates strongly with the percentage of fibrosis within the atria (Figure 5C). Although right atria (RA) from aged HFpEF animals also showed fibrotic remodeling compared with young (Supplemental Figure 2A), no changes were observed in the RA ADP_{90} or its heterogeneity (Supplemental Figure 2B–C). However, the level of atrial fibrosis is significantly higher in the LA (~16%) of aged HFpEF animals compared with RA (~10%), highlighting differential inter-atrial fibrosis remodeling. Together, our data provide several pieces of evidence that indicate potential atrial-dependent mechanisms by which AF can arise. To unequivocally validate our hypothesis, a rapid atrial pacing protocol was used to induce AF in *ex vivo* SAN/atrial tissue (Figure 5D). As shown in Figure 5D, aged animals had higher AF inducibility than young animals, as manifested by the formation of wavebreaks and initiation of spiral wave reentry.

Atrial fibrillation in aged rats is associated with enhanced atrial inflammation

The finding of elevated inflammatory biomarkers in the blood of aged animals (Figure 1G–I) prompted us to look specifically at inflammatory cells and cytokines in atrial tissue. In the

setting of an overall trend towards higher atrial cytokine levels in aged rats (Figure 5E), cytokine-induced neutrophil chemoattractants (CINC-2 and CINC-3) were significantly increased. We also found higher density of $CD68^+$ cells (macrophages) in aged animals compared with young (Figure 5F). At the cellular level, no changes in CD45 expression (indicative of white blood cells) were evident between the two age groups (Supplemental Figure 3A). Recently, inflammasome signaling has been implicated in AF patients[10]. Although protein levels of NLRP3 remained unchanged, levels of ASC and the active form of Caspase1 (Casp1-p20) were significantly upregulated in LA specimens from aged animals compared with young (Supplemental Figure 3A). Interestingly, only a subtle increase in cleaved gasdermin D (GSDMD, Supplemental Figure 3B) was observed, while the cleaved form of IL-1β and IL-18 were not changed between groups (Supplemental Figure 3B).

DISCUSSION

A growing body of evidence supports the notion that HFpEF is multifactorial in origin, which may explain the failure of pathway-selective agents in clinical trials of HFpEF patients[3]. Community-based studies demonstrate that most HFpEF patients are older, female, and likely to have multiple comorbidities, including hypertension, pulmonary disease, obesity, diabetes, and chronic kidney disease[5,19]. Here we have found that the high AF incidence in aged female rats is strongly associated with diastolic dysfunction and increased systemic and local inflammation, which may trigger local pro-inflammatory mediators.

Cardiac senescence strongly impacts the risk of cardiovascular disease[20,21]. Accordingly, aging-associated myocardial stiffness has been shown to be a major contributor to diastolic dysfunction,[22,23] which appears to be better-associated with AF than hypertension, which was only minimally elevated in our aged group. Further, our results support that enlargement of LA appendage correlates with higher AF prevalence[15], an arrhythmia which has been greatly associated with increased risk of all-cause mortality in HFpEF patients[2]. Although a previous study reported AF in aged male Fischer 344 rats[24], our study provides the first insight into AF mechanisms in animals with demonstrated HFpEF.

Most previous preclinical studies of HFpEF (including our own)[6,7,9,25] used animal models which incompletely replicate the chronological development of this disease and the striking epidemiological evidence of gender-related distribution[26]. In accordance with increased systemic inflammation in HFpEF patients[11], which potentiates AF[27], our findings provide novel evidence of local and systemic pro-inflammatory profiles, uncovering potential molecular therapeutic targets.

Inflammation in AF patients can arise from different sources, which can subsequently contribute to electrical remodeling and atrial fibrosis[27]. In fact, shorter AERP is an important substrate for AF-promoting reentry[15], while prolonged AERP has been shown in AF patients with sinus node dysfunction[28], as also observed in aged rats. In our study, β-AR stimulation abbreviated atrial APD[16,17], whereas its arrhythmogenic activity was only observed in aged animals. Moreover, extensive fibrotic remodeling in aged atria likely

contributes to APD instability and increased likelihood of ectopic or reentrant activity, thereby providing a critical substrate for AF[15]. However, the molecular basis of extracellular matrix remodeling deserves further investigation. Beyond systemic and local (atrial) inflammation, the excess adipose tissue reported here may also serve as an additional source of pro-inflammatory cytokines and mediators associated with metabolic disorders, which substantiate the inflammatory paradigm of HFpEF[29].

Chronic inflammation in the elderly population (inflammaging) is known to influence the age-related incidence of cardiovascular disease[21]. Despite lack of human HFpEF atrial biopsies supporting the proinflammatory milieu as a key mechanism underlying AF occurrence and maintenance, our results provide exploratory results supporting the role of systemic and atrial proinflammatory factors. Enhanced inflammasome signaling was recently described as a novel AF mechanism mediated by nonimmune cells[10]. As in the atria of patients with paroxysmal AF[10], here the abundance of NLRP3 remained unchanged, while the active form of Casp1 was significantly increased, indicating increased NLRP3 inflammasome activity. Although downstream effectors of inflammasome signaling, such as IL-1β and IL-18 did not change, they can generate the N-terminal GSDMD fragment, a pyroptosis executioner[18]. Thus, enhanced inflammasome/pyroptosis signaling in atrial HFpEF tissue may cause GSDMD-forming pores that allowing the release of other cytokines not investigated here and loss of plasma membrane integrity, which consequently compromise cellular excitability. Regardless, therapeutic strategies with NLRP3 inhibitors or cell pyroptosis suppressors warrant further investigation. Inflammasome signaling influences ion channel gene expression[10], and may activate danger-associated molecular factors to create heterogeneous repolarization and electrical conduction, which serve as a re-entrant substrate favoring AF maintenance.

STUDY LIMITATIONS

Our study has several limitations. First, further investigations are needed to establish (or reject) enhanced inflammasome signaling as a contributor AF propensity. Upstream and downstream factors of inflammasome signaling were not extensively investigated in the current study. Second, despite the certain relevance of investigating age/gender-related HFpEF animals with established disease, evaluation at different ages may allow the identification of triggers at an early stage of the pathology. Third, although electrical remodeling critically supports atrial rotors to initiate and maintain AF, we have not measured ion channel expression and/or function in our model. Moreover, the self-terminating nature of AF in this rodent model contrasts with human disease. Indeed, shorter atrial action potentials and refractory periods are known determinant factors (along with increased fibrosis and spatial APD heterogeneity) for re-entrant arrhythmias in AF[30]. However, conflicting results have been reported regarding adaptation to the rate of refractoriness during aging-related electrophysiologic changes[31]. Given the paucity of data regarding the electrophysiological basis of AF in human HFpEF, our findings have potential value in motivating such clinical studies.

CONCLUSION

In the present study, we have demonstrated that aged female animals exhibit diastolic dysfunction and other clinical features of HFpEF, including a propensity to AF. The arrhythmogenic mechanisms underlying this effect were associated with increased systemic inflammation, which may trigger local pro-inflammatory mediators, thereby causing abnormal atrial remodeling and favoring a substrate conducive to AF.

Supplementary Material

Refer to Web version on PubMed Central for supplementary material.

ACKNOWLEDGMENTS

We thank Lisa Trahan for editorial assistance and the National Institutes of Aging for providing aged rats. EM holds the Mark S. Siegel Family Distinguished Chair at Cedars-Sinai Medical Center.

SOURCES OF FUNDING

This research was supported by supported by National Institutes of Health (R01 HL124074 and R01 HL135866), the Peer-Reviewed Medical Research Program of the US Department of Defense (PR150620), American Heart Association (18CDA34110445), and the Cedars-Sinai Board of Governors.

REFERENCES

1. Cikes M, Claggett B, Shah AM, et al. Atrial Fibrillation in Heart Failure With Preserved Ejection Fraction: The TOPCAT Trial. JACC Heart Fail. 2018;6:689–697. [PubMed: 30007557]
2. Zakeri R, Chamberlain AM, Roger VL, et al. Temporal relationship and prognostic significance of atrial fibrillation in heart failure patients with preserved ejection fraction: a community-based study. Circulation. 2013;128:1085–1093. [PubMed: 23908348]
3. Dunlay SM, Roger VL, Redfield MM. Epidemiology of heart failure with preserved ejection fraction. Nat Rev Cardiol. 2017;14:591–602. [PubMed: 28492288]
4. Masoudi FA, Havranek EP, Smith G, et al. Gender, age, and heart failure with preserved left ventricular systolic function. J Am Coll Cardiol. 2003;41:217–223. [PubMed: 12535812]
5. Sharma K, Kass DA. Heart failure with preserved ejection fraction: mechanisms, clinical features, and therapies. Circ Res. 2014;115:79–96. [PubMed: 24951759]
6. Cho JH, Kilfoil PJ, Zhang R, et al. Reverse electrical remodeling in rats with heart failure and preserved ejection fraction. JCI Insight. 2018;3.
7. Gallet R, de Couto G, Simsolo E, et al. Cardiosphere-derived cells reverse heart failure with preserved ejection fraction (HFpEF) in rats by decreasing fibrosis and inflammation. JACC Basic Transl Sci. 2016;1:14–28. [PubMed: 27104217]
8. Shah KS, Xu H, Matsouaka RA, et al. Heart Failure With Preserved, Borderline, and Reduced Ejection Fraction: 5-Year Outcomes. J Am Coll Cardiol. 2017;70:2476–2486. [PubMed: 29141781]
9. Cho JH, Zhang R, Kilfoil PJ, et al. Delayed Repolarization Underlies Ventricular Arrhythmias in Rats With Heart Failure and Preserved Ejection Fraction. Circulation. 2017;136:2037–2050. [PubMed: 28974519]
10. Yao C, Veleva T, Scott L, et al. Enhanced Cardiomyocyte NLRP3 Inflammasome Signaling Promotes Atrial Fibrillation. Circulation. 2018;138:2227–2242. [PubMed: 29802206]
11. Hulsmans M, Sager HB, Roh JD, et al. Cardiac macrophages promote diastolic dysfunction. J Exp Med. 2018;215:423–440. [PubMed: 29339450]
12. Bowen TS, Brauer D, Rolim NPL, et al. Exercise Training Reveals Inflexibility of the Diaphragm in an Animal Model of Patients With Obesity-Driven Heart Failure With a Preserved Ejection Fraction. J Am Heart Assoc. 2017;6.

13. Westermann D, Lindner D, Kasner M, et al. Cardiac inflammation contributes to changes in the extracellular matrix in patients with heart failure and normal ejection fraction. Circ Heart Fail. 2011;4:44–52. [PubMed: 21075869]
14. Glezeva N, Voon V, Watson C, et al. Exaggerated inflammation and monocytosis associate with diastolic dysfunction in heart failure with preserved ejection fraction: evidence of M2 macrophage activation in disease pathogenesis. J Card Fail. 2015;21:167–177. [PubMed: 25459685]
15. Nattel S, Burstein B, Dobrev D. Atrial remodeling and atrial fibrillation: mechanisms and implications. Circ Arrhythm Electrophysiol. 2008;1:62–73. [PubMed: 19808395]
16. Yeh Y-H, Ehrlich JR, Qi X, et al. Adrenergic control of a constitutively active acetylcholine-regulated potassium current in canine atrial cardiomyocytes. Cardiovasc Res. 2007;74:406–415. [PubMed: 17343836]
17. Lang D, Sulkin M, Lou Q, et al. Optical mapping of action potentials and calcium transients in the mouse heart. J Vis Exp. 2011;
18. Shi J, Zhao Y, Wang K, et al. Cleavage of GSDMD by inflammatory caspases determines pyroptotic cell death. Nature. 2015;526:660–665. [PubMed: 26375003]
19. McHugh K, DeVore AD, Wu J, et al. Heart Failure With Preserved Ejection Fraction and Diabetes: JACC State-of-the-Art Review. J Am Coll Cardiol. 2019;73:602–611. [PubMed: 30732715]
20. Grigorian-Shamagian L, Liu W, Fereydooni S, et al. Cardiac and systemic rejuvenation after cardiosphere-derived cell therapy in senescent rats. Eur Heart J. 2017;38:2957–2967. [PubMed: 29020403]
21. Gude NA, Broughton KM, Firouzi F, et al. Cardiac ageing: extrinsic and intrinsic factors in cellular renewal and senescence. Nat Rev Cardiol. 2018;15:523–542. [PubMed: 30054574]
22. Zile MR, Baicu CF, Ikonomidis JS, et al. Myocardial stiffness in patients with heart failure and a preserved ejection fraction: contributions of collagen and titin. Circulation. 2015;131:1247–1259. [PubMed: 25637629]
23. Bustamante M, Garate-Carrillo A, R Ito B, et al. Unmasking of oestrogen-dependent changes in left ventricular structure and function in aged female rats: a potential model for pre-heart failure with preserved ejection fraction. J Physiol (Lond). 2019;
24. Hayashi H, Wang C, Miyauchi Y, et al. Aging-related increase to inducible atrial fibrillation in the rat model. J Cardiovasc Electrophysiol. 2002;13:801–808. [PubMed: 12212701]
25. Cho JH, Zhang R, Aynaszyan S, et al. Ventricular Arrhythmias Underlie Sudden Death in Rats With Heart Failure and Preserved Ejection Fraction. Circ Arrhythm Electrophysiol. 2018;11:e006452. [PubMed: 30030266]
26. Lam CSP, Carson PE, Anand IS, et al. Sex differences in clinical characteristics and outcomes in elderly patients with heart failure and preserved ejection fraction: the Irbesartan in Heart Failure with Preserved Ejection Fraction (I-PRESERVE) trial. Circ Heart Fail. 2012;5:571–578. [PubMed: 22887722]
27. Hu Y-F, Chen Y-J, Lin Y-J, et al. Inflammation and the pathogenesis of atrial fibrillation. Nat Rev Cardiol. 2015;12:230–243. [PubMed: 25622848]
28. Uhm J-S, Mun H-S, Wi J, et al. Prolonged atrial effective refractory periods in atrial fibrillation patients associated with structural heart disease or sinus node dysfunction compared with lone atrial fibrillation. Pacing Clin Electrophysiol. 2013;36:163–171. [PubMed: 23121003]
29. Paulus WJ, Tschöpe C. A novel paradigm for heart failure with preserved ejection fraction: comorbidities drive myocardial dysfunction and remodeling through coronary microvascular endothelial inflammation. J Am Coll Cardiol. 2013;62:263–271. [PubMed: 23684677]
30. Workman AJ, Kane KA, Rankin AC. The contribution of ionic currents to changes in refractoriness of human atrial myocytes associated with chronic atrial fibrillation. Cardiovasc Res. 2001;52:226–235. [PubMed: 11684070]
31. Xu G-J, Gan T-Y, Tang B-P, et al. Age-related changes in cellular electrophysiology and calcium handling for atrial fibrillation. J Cell Mol Med. 2013;17:1109–1118. [PubMed: 23837844]

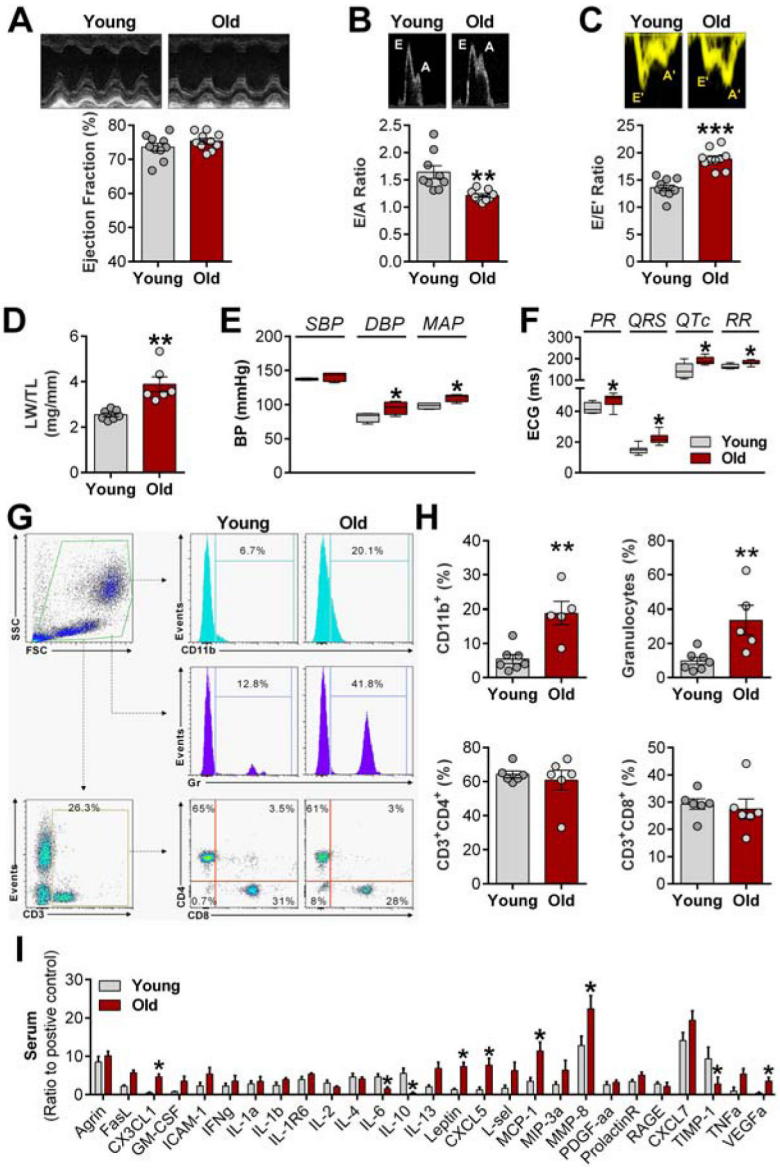

Figure 1. Aging-related diastolic dysfunction is associated with increased proinflammatory stress.

A, Representative echocardiography images (*top*) of ejection fraction analysis (*bottom*); **B**, Representative images (*top*) of pulse-wave Doppler showing E (early filling) and A (atrial filling) wave changes (*bottom*); **C**, Representative images (*top*) of tissue Doppler describing E' and A' wave changes (*bottom*); **D**, LW/TL: lungs weight/tibia length ratio; **E**, Non-invasive blood pressure (SAP: systolic, DAP: diastolic, and MAP: mean arterial pressure, n= 5 animals each group) measurements. **F**, Electrocardiograms intervals analyses (n= 8 animals each group); **G**, Representative flow cytometry histograms of CD11b+ cells and granulocytes; **H**, Quantification of flow cytometry data. **I**, Expression of proinflammatory and profibrotic cytokines in serum (n= 4 animals each group). Data are expressed as mean ± SEM. Unpaired Student's t-test. *P<0.05, **P<0.01, ***P<0.001 vs. young females.

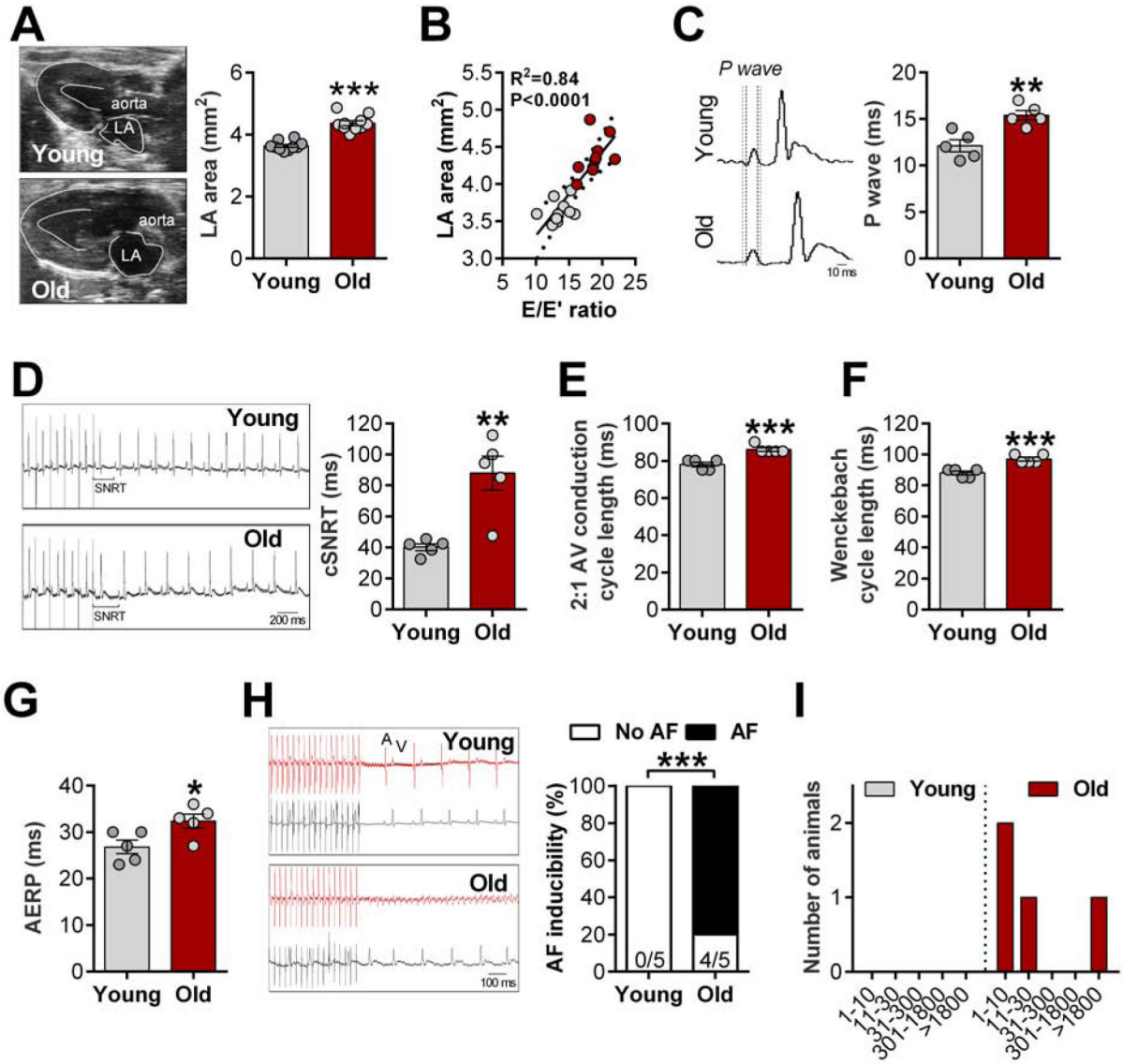

Figure 2. Atrial enlargement and SAN/AV dysfunction underlie high atrial fibrillation incidence in aged rats.

A, Representative B-mode echocardiography recordings (*left*) and quantification of left atrial (LA) area (*right*); **B**, Relationship between E/E' ratio and LA area, data fit by linear regression; 95% confidence limits. **C**, Representative ECG recordings (*left*), dashed lines highlight prolonged P wave duration in aged animals and quantification of P wave duration (*right*); **D**, Representative ECG recordings (*left*) and quantification of corrected sinoatrial node recovery time (cSNRT, *right*); **E-F**, 2:1 AV conduction cycle length (**E**) and Wenckebach cycle length (**F**) assess AV node function; **G**, Quantification of atrial effective refractory period (AERP); **H**, Representative simultaneous recordings of intracardiac potentials (red line) and surface ECG (lead II, black line) protocol used to induce atrial fibrillation (AF, *left*) and incidence of pacing-induced AF (*right*); **I**, Duration of AF in young and aged animals. Data are expressed as mean ± SEM. Unpaired Student's t-test. χ2-test without Yates correction (**H**). *P<0.05, **P<0.01, ***P<0.001 vs. young females.

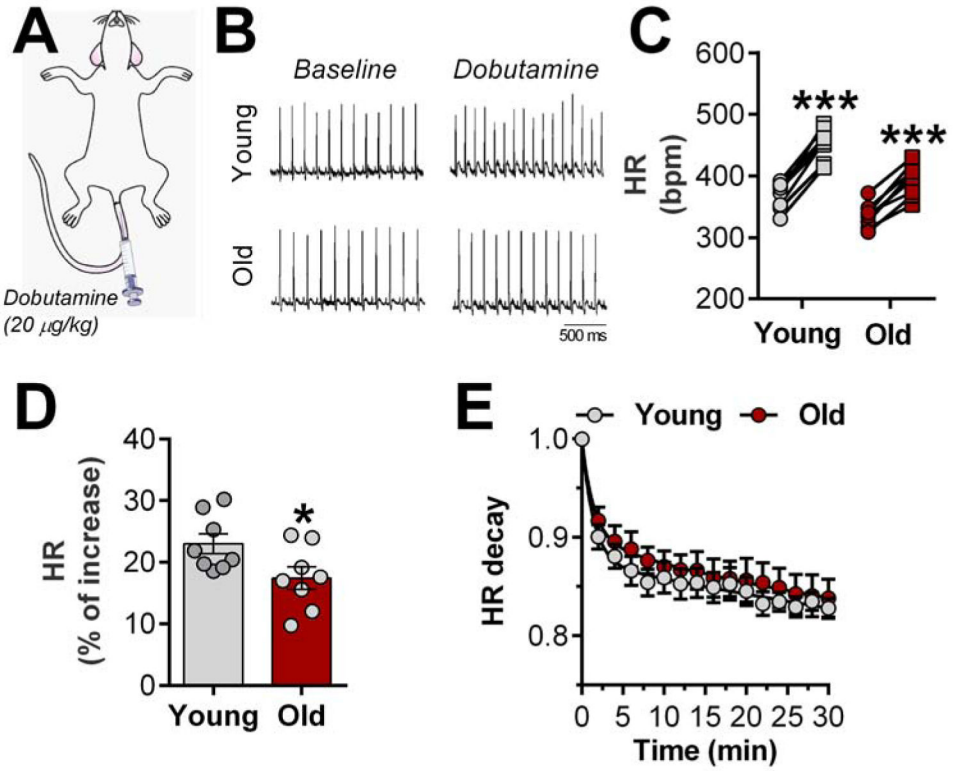

Figure 3. Chronotropic reserve is impaired in aged rats.

A, *In vivo* dobutamine stress was used to determine the chronotropic reserve in young and aged animals; Representative ECG recordings (**B**) and quantification of β-adrenergic-induced heart rate (HR) increase (**C**, circle: baseline and square: dobutamine-induced HR response); **D**, β-adrenergic responsiveness in both groups; **E**, HR recovery time after maximal effect of dobutamine. Data are expressed as individual values (before-after, **C**) and mean ± SEM. Paired (**C**) and unpaired Student's t-test (**D**). Double-exponential fit of HR decay phase was used. ***P<0.01 vs. baseline and *P<0.05 vs. young females.

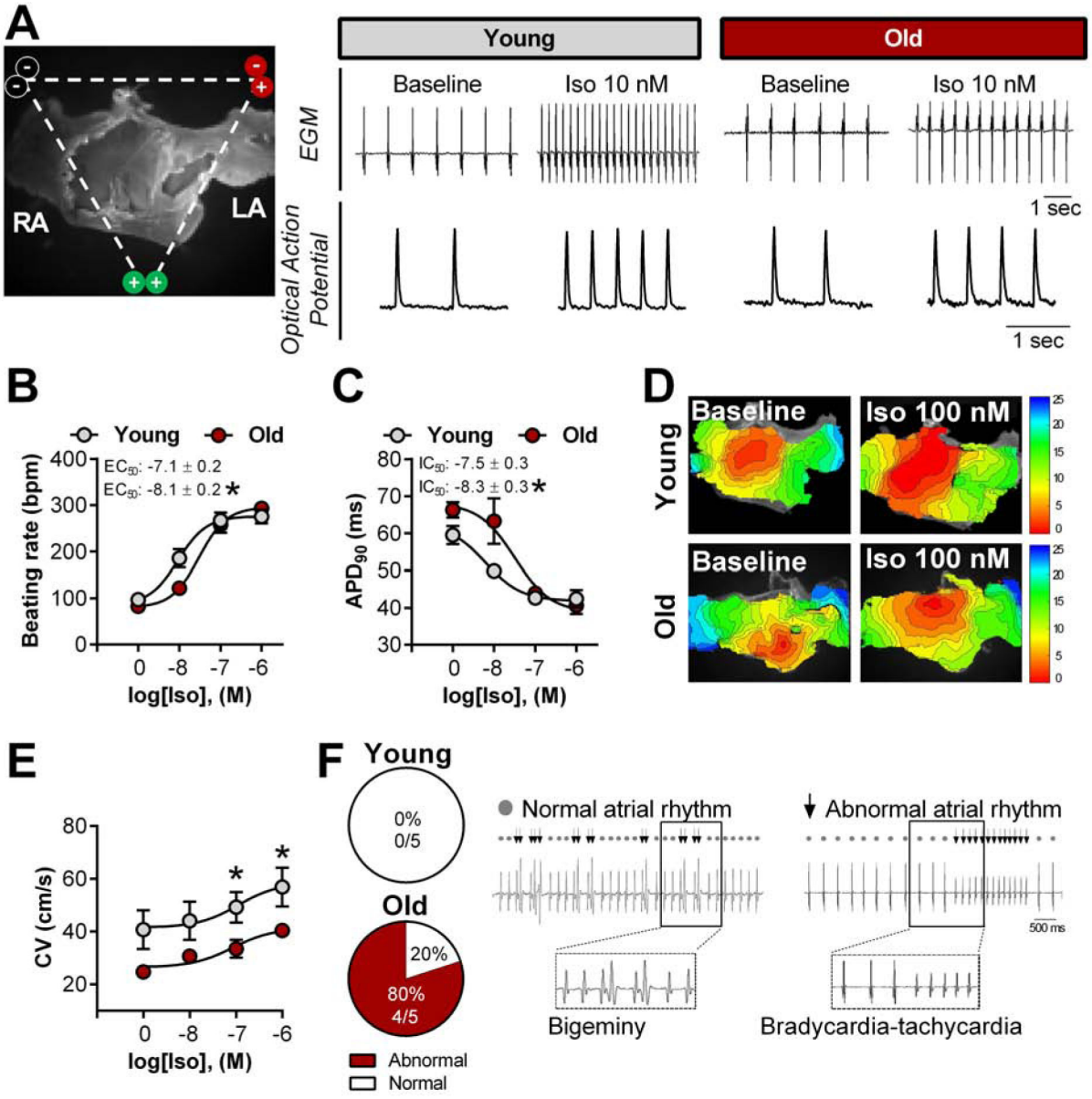

Figure 4. Slowed conduction velocity underlies β-adrenergic-induced abnormal rhythm in aged rats.

A, Representative image of electrodes placement surrounding the *ex vivo* SAN/atrial tissue loaded with a voltage-sensitive dye (*left*) and simultaneous recordings of electrograms (EGM) and optical action potential in the left atrial (LA) appendage of young and aged females rats under baseline and isoproterenol (Iso) conditions (*right*); Spontaneous sinus rhythm and concentration-response curve for isoproterenol was applied to evaluate *ex vivo* beating rate (**B**) and action potential duration at 90% (APD_{90}) (**C**). **D**, Representative images of isochronal voltage maps and conduction velocity (CV, **E**) in the LA; **F**, Occurrence of abnormal rhythm throughout the dose-response curve to Iso (*left*) and representative EGM traces (*right*). Data are expressed as mean ± SEM. Sigmoidal dose-response curve fits were generated to calculate the half maximal effective (EC50) and inhibitory (IC50)

concentration. χ2-test without Yates correction (**F**). n= 5 animals each group. *P<0.05 vs. young females.

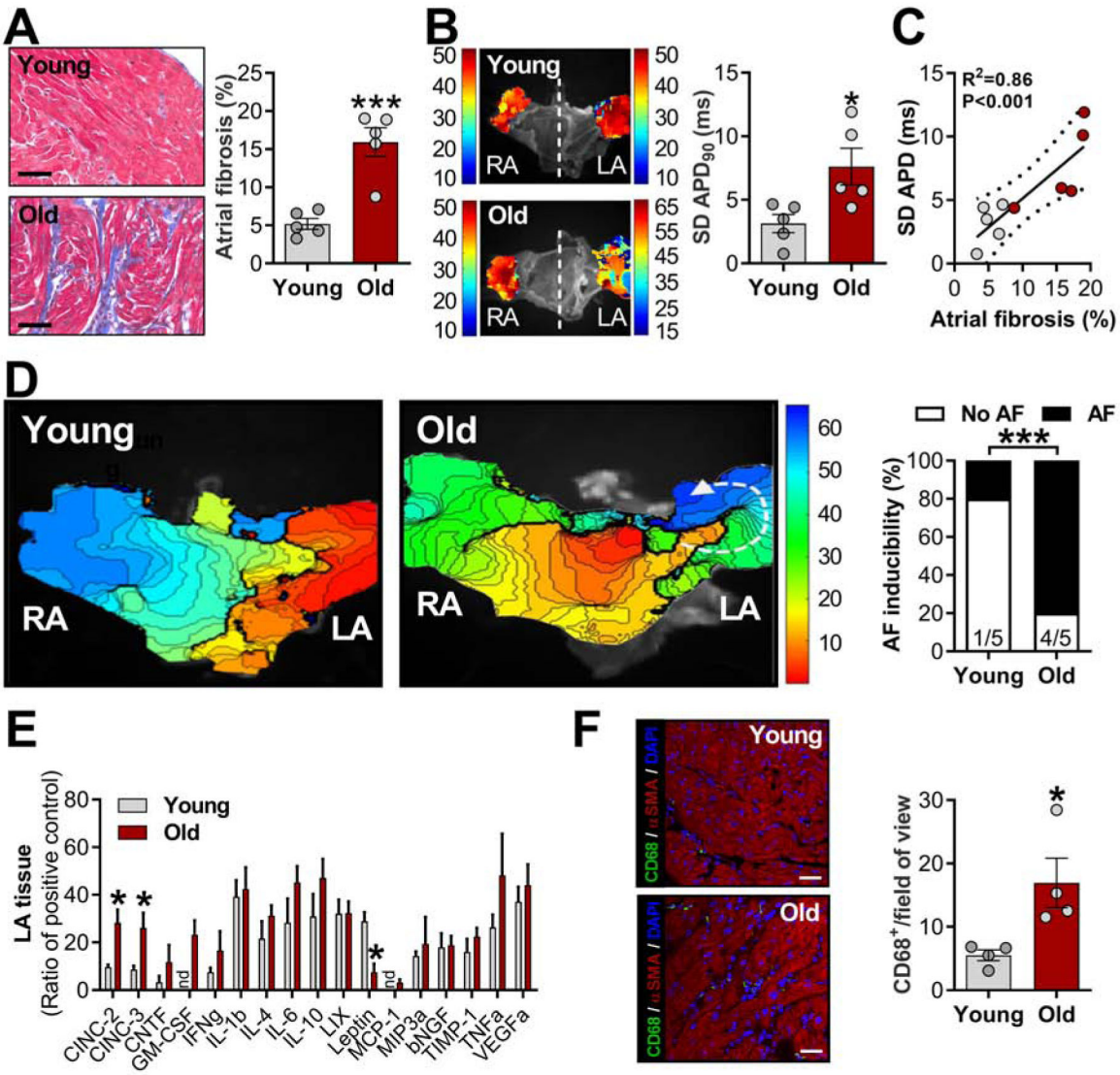

Figure 5. Increased atrial fibrosis and inflammation are critical substrates for atrial fibrillation-promoting reentry circuit in aged rats.

A, Representative Masson's trichrome-stained sections of left atrial (LA) tissue (*left*) and quantification (*right*); **B**, Representative atrial action potential duration (APD) maps of young and aged females (*left*) and standard deviation (SD) of APD 90% (APD_{90} dispersion) measured at three random regions in LA appendage (*right*); **C**, Relationship between atrial fibrosis and area, data fit by linear regression; 95% confidence limits. **D**, Representative images of isochronal voltage maps (*left*) and incidence of atrial fibrillation (AF) obtained *ex vivo* (*right*). **E**, Cytokines levels in LA samples (nd= not detected, n= 4 animals each group); **F**, CD68 immunostaining of LA (*left*; scale bar: 20 m) and pooled data from $CD68^+$ cells within the LA tissue (*right*). Data are expressed as mean ± SEM. Unpaired Student's t-test. $\chi 2$-test without Yates correction (**E**). *P<0.05 and ***P<0.001 vs. young females.

Table 1.

Echocardiographic and anatomical characteristics of young and old female rats.

	Young	Old
Echocardiographic Parameters		
ESD (mm)	3.05 ± 0.16	3.46 ± 0.18
EDD (mm)	5.46 ± 0.14	6.37 ± 0.16***
LVAWs (mm)	0.97 ± 0.05	1.23 ± 0.05**
LVAWd (mm)	0.79 ± 0.04	0.93 ± 0.03*
LVPWs (mm)	1.01 ± 0.04	1.30 ± 0.05***
LVPWd (mm)	0.79 ± 0.04	0.92 ± 0.03*
IVS (mm)	0.83 ± 0.03	1.25 ± 0.05***
Anatomical Parameters		
HW/TL (mg/mm)	1.69 ± 0.053	2.52 ± 0.14***
AW/TL (mg/mm)	0.22 ± 0.016	0.29 ± 0.017*
Adipose tissue/BW (g/g)	17.01 ± 1.27	29.15 ± 0.27***
Exercise capacity (meters)	390.6 ± 38.82	191.8 ± 9.56**

EDD, end-diastolic diameter; ESD, end-systolic diameter; LVAWd, left-ventricular end-diastolic anterior wall thickness; LVAWs, left-ventricular end-systolic anterior wall thickness; LVPWd, left-ventricular end-diastolic posterior wall thickness; LVPWs, left-ventricular end-systolic posterior wall thickness; IVS, interventricular septum; HW, heart weight; AW, atria weight; TL, tibia length; BW, body weight. Data are expressed as mean ± SEM. Unpaired Student's t-test. n= 10 animals each group.

* P<0.05,

** P<0.01,

*** P<0.05 vs. aged females.